An Integrated Molecular Orbital + Molecular Orbital (IMOMO) Study of the O + H−R → OH + R$^\bullet$ Reaction Class

Qian Shu Li,*,[†,‡] Qinghua Zhao,[†] and Shaowen Zhang[†]

School of Science, Beijing Institute of Technology, Beijing 100081, People's Republic of China, and Institute of Theoretical Chemistry, State Key Laboratory of Theoretical and Computational Chemistry, Jilin University, Changchun 130023, People's Republic of China

Received: March 30, 2004; In Final Form: June 1, 2004

We investigate the O + H−R → OH + R$^\bullet$ reaction class by employing the integrated molecular orbital + molecular orbital (IMOMO) methodology. The QCISD(T), MP4, and MP2 methods are employed as the high-level theories in the IMOMO method based on the geometries optimized at the BH&HLYP and MPW1K methods. The results show that the energies predicted from both QCISD(T) and MP4 calculations can reasonably be reproduced by the IMOMO method. In particular, the IMOMO method yields the mean absolute deviation of about 1 kcal/mol in reaction energies and less than 0.4 kcal/mol in classical barrier heights. The predicted thermal rate constants are in good agreement with the available experimental data. This approach has been further proven to be powerful tools for studying reactions involving large molecular systems.

I. Introduction

With the advent of computational science, the interests of computational chemistry are being shifted toward more and more realistic models and larger molecular systems. However, to obtain accurate electronic structure and energetic information for the large molecular systems, one has to employ the expensive but more reliable ab initio molecular orbital (MO) theory such as the MP4 or QCISD(T) level. Such calculations are computationally expensive for systems that have more than four non-hydrogen atoms. A variety of approaches has been developed for reducing computational cost. For example, Morokuma and co-workers[1−4] have presented an integrated molecular orbital + molecular orbital (IMOMO) method. This method considers a small "model" system within a large "real" system, applies a "higher"-level calculation for the model system and a "lower"-level calculation for the real system, and integrates them to define a total energy of the real system. This method has been shown to be quite valuable so far.[5,6] For the same purpose, Truong and co-workers[7−9] have proposed a reaction-class approach. The central idea is from recognizing that reactions that have the same reactive moiety have similar features on their potential-energy surface along the particular reaction path direction. Therefore, the certain potential information from the principal reaction (the smallest reaction in the class) can be transferred to larger reactions in the same class without having to calculate it explicitly. Furthermore, Truong et al. have combined the reaction class approach with the IMOMO methodology for improving energetic information of chemical reactions.[10,11] This approach has been successfully applied to hydrogen abstraction reactions of hydrocarbons by the hydrogen atom, and yields average unsigned errors of about 1 kcal/mol in the reaction energies and about 0.2 kcal/mol in the barrier heights for saturated hydrocarbon systems. After that, they calculated the thermal rate constants of hydrogen abstraction reactions of hydrogen atom with fluoromethanes (CH_3F, CH_2F_2, and CHF_3) based on the above approach.[11] The results have shown that the approach can reduce computational cost while maintaining an acceptable accuracy.

In this paper, we test the validity of the IMOMO methodology in the hydrogen abstraction reactions of hydrocarbons by oxygen atom, which is an important class of reactions in combustion chemistry.

II. Methodology

A. The IMOMO Methodology. In the IMOMO approach, the total energy of a large "real" system is defined as[3]

$$E(\text{IMOMO}) = E(\text{high,model}) + [E(\text{low,real}) - E(\text{low,model})] \quad (1)$$

where "high" and "low" refer to levels of MO calculation, while "real" and "model" refer to the large "real" system and the small "model" system, respectively. In this approach, the geometries of the species of the "model" reaction and the "real" reaction are optimized at the "low" level of theory that demands less computational resources. The high-level energy refinement is performed only for the "model" reaction, and this also needs relatively small computational demands due to the small size of the "model" reaction. Obviously, the IMOMO method duplicates the correlation energy of the "model" system to the "real" system. Because of the difference of sizes between the "model" system and the "real" system, E(IMOMO) is not an accurate estimation of the energy of the "real" system at the "high" level of theory. However, in some circumstance, it is the relative energy but not the absolute energy of the system that is of interest. For instance, when we calculate the rate constants of a reaction, the reaction barrier, namely, the relative energy between the transition state and the reactant, is of our interest. In some cases when we calculate relative energies such as reaction barrier, the difference of correlation energy caused by size might be canceled and the IMOMO method is very useful. The IMOMO method is of particular interest for the

---

* To whom correspondence may be addressed. E-mail: qsli@bit.edu.cn. Fax: +86-10-68912665. Tel.: +86-10-68912665.

[†] Beijing Institute of Technology.

[‡] Jilin University.

10.1021/jp048606n CCC: $27.50

reaction class theory. Truong and co-workers[10,11] have demonstrated the validity of the IMOMO method for the hydrogen abstraction reactions by a hydrogen atom, in which the reactions generally have early transition states. In the present study, we expect to show the validity of the IMOMO method in the hydrogen abstraction reaction by an oxygen atom.

The reactions considered in this paper are

$$O + H{-}CH_2CH_3 \rightarrow OH + CH_3CH_2 \qquad (R1)$$

$$O + H{-}CH_2CH_2CH_3 \rightarrow OH + CH_3CH_2CH_2 \qquad (R2)$$

$$O + H{-}CH(CH_3)_2 \rightarrow OH + (CH_3)_2CH \qquad (R3)$$

$$O + H{-}CH_2F \rightarrow OH + CH_2F \qquad (R4)$$

$$O + H{-}CHF_2 \rightarrow OH + CHF_2 \qquad (R5)$$

$$O + H{-}CF_3 \rightarrow OH + CF_3 \qquad (R6)$$

$$O + H{-}CH_2C_3H_7 \rightarrow OH + C_3H_7CH_2 \qquad (R7)$$

$$O + H{-}CH(CH_3)C_2H_5 \rightarrow OH + C_2H_5(CH_3)CH \qquad (R8)$$

$$O + H{-}C(CH_3)_3 \rightarrow OH + (CH_3)_3C \qquad (R9)$$

The above reactions have the same "model" system for high-level calculations, namely, the $O + H{-}CH_3 \rightarrow OH + CH_3$ reaction is the "model" reaction of this class. Reactions R1, R2, R4, and R7 involve hydrogen abstraction from primary carbons, while reactions R3, R5, and R8 involve hydrogen abstraction from secondary carbons, and reactions R6 and R9 are tertiary hydrogen abstraction. Therefore, by calculating the energies of the hydrogen abstractions from primary, secondary, and tertiary carbons in the real systems listed above, we can examine the effect of the IMOMO method of all these types of reactions.

B. Thermal Rate Constant. At present time, thermal rate constants can be accurately evaluated using some sophisticated methods such as the canonical variational transition state theory (CVT).[12−18] The quantum transmission coefficients can be calculated by the small curvature tunneling (SCT) method.[16,19] For the present study, we only perform a cursory comparison between the experimental rate constants and those calculated using the transition state theory to show the validity of the IMOMO theory in predicting reaction barriers. Within the transition state theory (TST) framework,[20] the thermal rate constant of a reaction can be expressed as

$$k(T) = \kappa(T)\sigma \frac{k_B T}{h} \frac{Q^{\ddagger}}{Q^{R}} \exp\left(-\frac{\Delta V^{\ddagger}}{k_B T}\right) \qquad (2)$$

where $\kappa(T)$ is the transmission coefficient accounting for the quantum mechanical tunneling effects, σ is the reaction symmetry number, $Q^{\ddagger}$ is the total partition functions of the transition state, Q^{R} is the total partition functions (per unit volume) of the reactants, $\Delta V^{\ddagger}$ is the classical barrier height, T is the temperature, and k_B and h are the Boltzmann and Plank constants, respectively.

The above reactions are hydrogen abstraction reactions with apparent barrier height in which the tunneling effect is significant for predicting rate constants. To obtain an accurate estimation of tunneling effects, we need to use the more sophisticated SCT method.[16,19] However, we hope to provide a practical method to easily estimate the rate constants of large reaction systems. Thus, in the present study, we only use the Eckart method[21] to estimate the transmission coefficient.

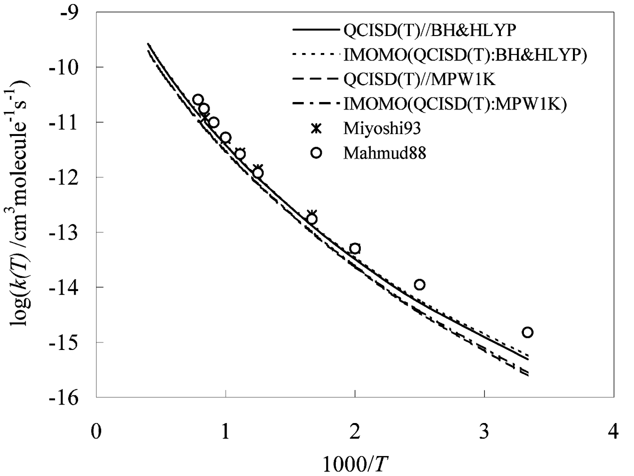

Figure 1. Arrhenius plots of the calculated rate constants at the QCISD(T)//BH&HLYP, IMOMO(QCISD(T):BH&HLYP), QCISD(T)//MPW1K, and IMOMO(QCISD(T):MPW1K) levels of theory for the $O + H{-}CH_2CH_3 \rightarrow OH + CH_3CH_2$ reaction along with available experimental data.

C. Computational Details. In an earlier IMOMO study of the $H + H{-}R \rightarrow H_2 + R^{\bullet}$ reaction class by Truong and co-workers,[22,23] they showed that the hybrid DFT method BH&HLYP/cc-pVDZ provides good predictions of geometries of the reactants, transition states, and products. Recently, Truhlar and co-workers developed a new hybrid DFT method MPW1K for predicting geometries and energetic and kinetics data of reactions.[24−26] These hybrid DFT methods have proven their efficiency and accuracy in predicting geometries of similar species to the present study. Therefore, the two methods are employed as low levels of theory in the IMOMO approach to optimize the geometries of the species in all the reactions presented in this study. For comparison purpose, we employed different high-level methods and basis sets to test the IMOMO approach. When the BH&HLYP/cc-pVDZ method is used as a low level of theory, the QCISD(T) and MP4 levels of theory with the cc-pVTZ basis set, and MP2 level of theory with the cc-pVQZ basis set are used as the high-level of theory, and denoted as high: BH&HLYP (here high indicates the QCISD(T), MP4, and MP2 levels, respectively, the same as below). Similarly, when the MPW1K/6-31+G(d,p) method is used as a low level of theory, the QCISD(T) and MP4 levels of theory with the 6-311++G(2df,p) basis set and MP2 level of theory with the 6-311++G(3df,2pd) basis set are used as the high level of theory, and denoted as high: MPW1K. We adopt the 6-31+G(d,p) basis set for the MPW1K calculation due to the fact that this method has been proven that it can provide good prediction of geometries of stable molecules and transition states.[27,28] To explain the IMOMO approach discussed in the earlier section with these MO calculation methods, we take an example with the MP4/cc-pVTZ as the high-level of theory and BH&HLYP/cc-pVDZ as the low level of theory; the energy of the IMOMO calculation can be expressed as

$$\begin{aligned} E(\text{IMOMO}) = \text{IMOMO}(\text{MP4:BH\&HLYP}) = \\ E(\text{MP4/cc-pVTZ//BH\&HLYP/cc-pVDZ;model}) + \\ [E(\text{BH\&HLYP/cc-pVDZ;real}) - \\ E(\text{BH\&HLYP/cc-pVDZ;model})] \end{aligned}$$

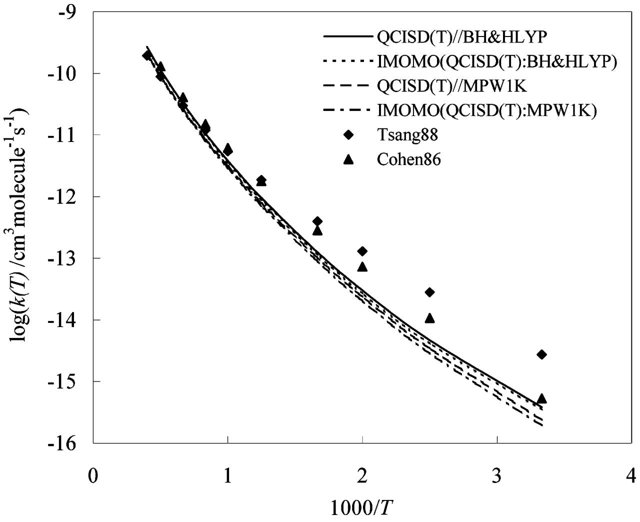

Figure 2. Arrhenius plots of the calculated rate constants at the QCISD(T)//BH&HLYP, IMOMO(QCISD(T):BH&HLYP), QCISD(T)//MPW1K, and IMOMO(QCISD(T):MPW1K) levels of theory for the O + $H{-}CH_2CH_2CH_3 \rightarrow OH + CH_3CH_2CH_2$ reaction.

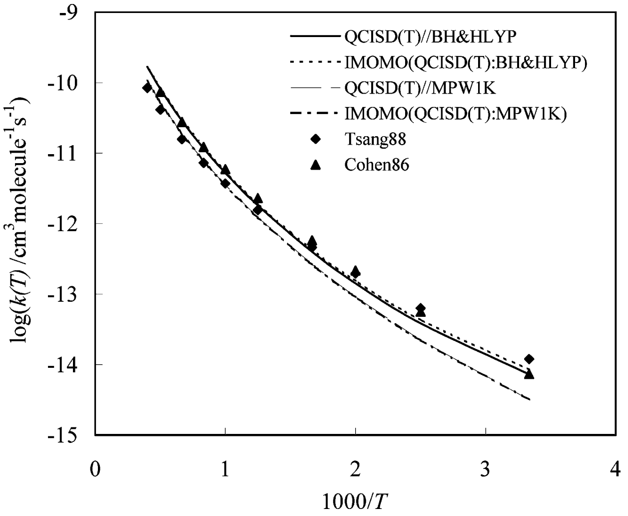

Figure 3. Arrhenius plots of the calculated rate constants at the QCISD(T)//BH&HLYP, IMOMO(QCISD(T):BH&HLYP), QCISD(T)//MPW1K, and IMOMO(QCISD(T):MPW1K) levels of theory for the O + $H{-}CH(CH_3)_2 \rightarrow OH + (CH_3)_2CH$ reaction.

The rests may be deduced by analogy. All of the electronic structure calculations are done using the Gaussian 98 Program.[29]

III. Results and Discussion

Tables 1, 2, and 3 show the comparison of reaction energies, classical barrier heights, and absolute deviations between the high level results and the IMOMO results at the QCISD(T):BH&HLYP, MP4:BH&HLYP, and MP2:BH&HLYP levels of theory, respectively. From these tables, we can see that the QCISD(T):BH&HLYP method predicts the best reaction energies and barrier heights among the three methods with the mean absolute deviation (MAD) of 0.87 kcal/mol for reaction energies and 0.14 kcal/mol for barrier heights. The MAD of the MP4:BH&HLYP method is 1.07 kcal/mol for reaction energies and 0.28 kcal/mol for barrier heights. Thus, both the QCISD(T):BH&HLYP and MP4:BH&HLYP methods can provide good approximations for reaction energies and barrier heights despite the fact that the MAD of barrier heights of the MP4:BH&HLYP method is twice that of the QCISD(T):BH&HLYP method. The MAD of the MP2:BH&HLYP method is 1.26 kcal/mol for reaction energies and 0.97 kcal/mol for barrier heights. Although the MAD of reaction energies of the MP2:BH&HLYP method is close to that of the QCISD(T):BH&HLYP and MP4:BH&HLYP methods, its MAD of barrier heights seems too large compared to the later two methods. It is interesting that the MAD of barrier heights is smaller than that of reaction energies for all the IMOMO methods. This is caused by the fact that the absolute deviations ($\Delta\Delta E$ in the tables) of barrier heights are almost identical for the primary, secondary, and tertiary hydrogen abstractions in contrast to the fact that the $\Delta\Delta E$ of reaction energies has systematic error between different types of hydrogen abstractions. In particular, the $\Delta\Delta E$ of reaction energies of secondary hydrogen abstractions is about 0.8 kcal/mol larger than that of primary hydrogen abstractions; similarly, the $\Delta\Delta E$ of reaction energies of tertiary hydrogen abstractions is about 0.8 kcal/mol larger than that of secondary hydrogen abstractions. Thus, eq 1 is a good estimation of barrier heights for the O + H−R reaction class. However, it might be more accurate in predicting reaction energies of the O + H−R reaction class if we put an additional constant (0.8 kcal/mol, for example) into eq 1. The fact that the IMOMO method

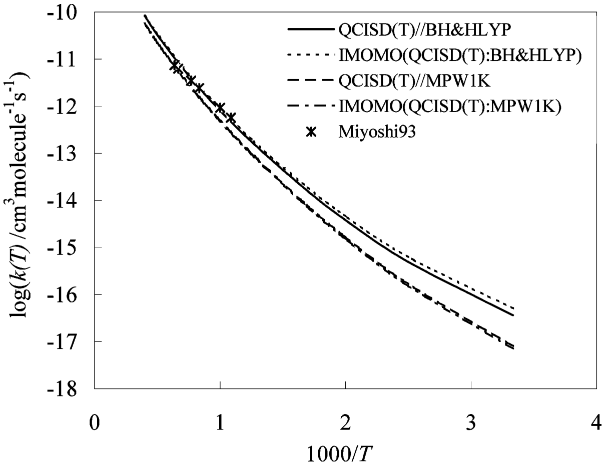

Figure 4. Arrhenius plots of the calculated rate constants at the QCISD(T)//BH&HLYP, IMOMO(QCISD(T):BH&HLYP), QCISD(T)//MPW1K, and IMOMO(QCISD(T):MPW1K) levels of theory for the O + $H{-}CH_2F \rightarrow OH + CH_2F$ reaction.

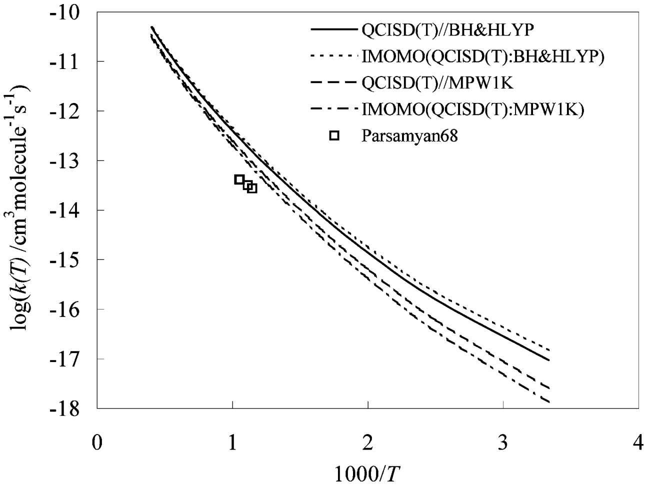

Figure 5. Arrhenius plots of the calculated rate constants at the QCISD(T)//BH&HLYP, IMOMO(QCISD(T):BH&HLYP), QCISD(T)//MPW1K, and IMOMO(QCISD(T):MPW1K) levels of theory for the O + $H{-}CHF_2 \rightarrow OH + CHF_2$ reaction.

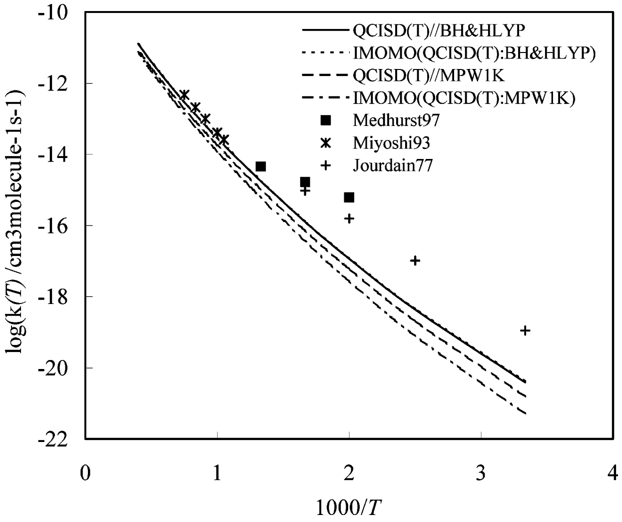

Figure 6. Arrhenius plots of the calculated rate constants at the QCISD(T)//BH&HLYP, IMOMO(QCISD(T):BH&HLYP), QCISD(T)//MPW1K, and IMOMO(QCISD(T):MPW1K) levels of theory for the O + H−CF_3 → OH + CF_3 reaction.

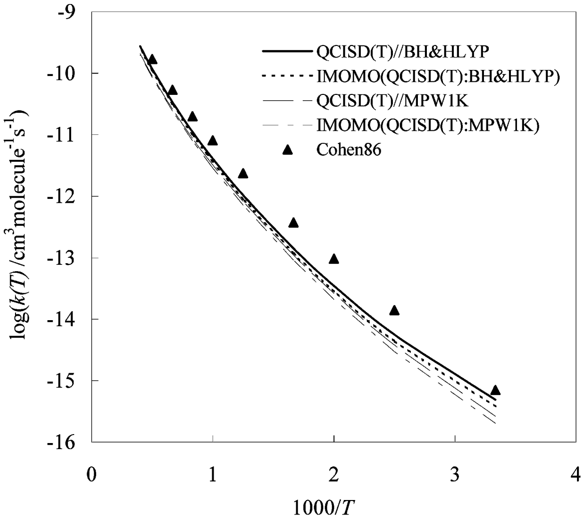

Figure 7. Arrhenius plots of the calculated rate constants at the QCISD(T)//BH&HLYP, IMOMO(QCISD(T):BH&HLYP), QCISD(T)//MPW1K, and IMOMO(QCISD(T):MPW1K) levels of theory for the O + H−$CH_2C_3H_7$ → OH + $C_3H_7CH_2$ reaction.

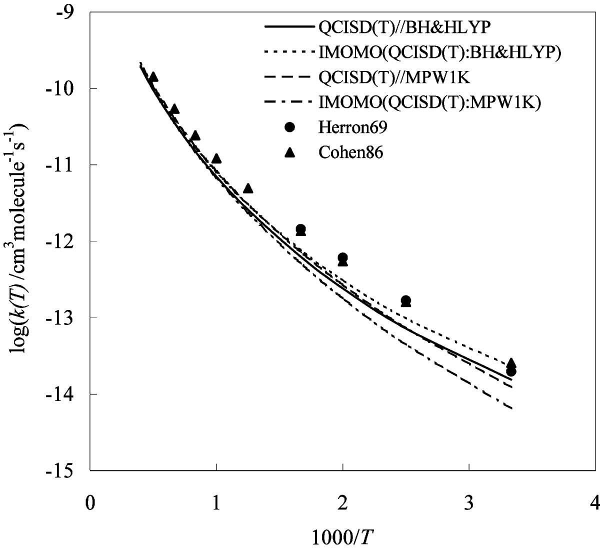

Figure 8. Arrhenius plots of the calculated rate constants at the QCISD(T)//BH&HLYP, IMOMO(QCISD(T):BH&HLYP), QCISD(T)//MPW1K, and IMOMO(QCISD(T):MPW1K) levels of theory for the O + H−CH-$(CH_3)C_2H_5$ → OH + C_2H_5 $(CH_3)CH$ reaction.

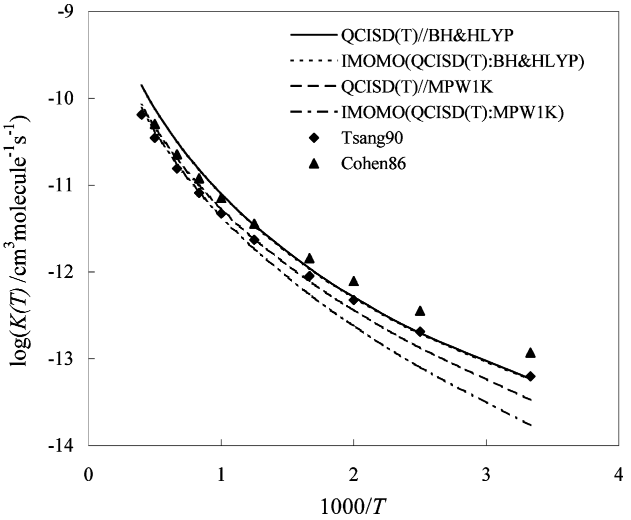

Figure 9. Arrhenius plots of the calculated rate constants at the QCISD(T)//BH&HLYP, IMOMO(QCISD(T):BH&HLYP), QCISD(T)//MPW1K, and IMOMO(QCISD(T):MPW1K) levels of theory for the O + H−$C(CH_3)_3$ → OH + $(CH_3)_3C$ reaction.

provides better prediction for barrier heights than for reaction energies is caused by the approximation of the IMOMO method. As discussed in the methodology section, the IMOMO method duplicates the correlation energy of the "model" system to the "real" system. When we calculate relative energies for the "real" system using the IMOMO method, we assume that the contribution of correlation energy in relative energy of the "model" system is the same as that of the "real" system. For the present reaction class, since the transition state of each reaction appears early on the potential-energy surface, the structure of the transition state is close to the reactants. Thus, the difference of correlation energies between the transition state and reactants of the "model" reaction is close to those of the "real" reactions, and thus the IMOMO method can provide a good prediction of barrier heights. However, the structures of the products are not so close to those of the reactants for each reaction in the reaction class. The difference of correlation energy between the reactants and products of the "model" reaction is somewhat different from those of the "real" reactions, and thus the IMOMO method gives a larger $\Delta\Delta E$ in predicting reaction energies. Fortunately, the $\Delta\Delta E$ of the IMOMO method in predicting reaction energy is still in the acceptable range.

Tables 4, 5, and 6 list the comparison of reaction energies, classical barrier heights, and absolute deviations between the high-level results and the IMOMO results at the QCISD(T):MPW1K, MP4:MPW1K, and MP2:MPW1K levels of theory, respectively. Obviously, the accuracy of the predicted reaction energies and barrier heights from these IMOMO methods are in accordance with those from the corresponding IMOMO methods of QCISD(T):BH&HLYP, MP4:BH&HLYP, and MP2:BH&HLYP since the high-level theory of the corresponding IMOMO methods (for example, QCISD(T):MPW1K and QCISD(T):BH&HLYP) are identical despite the fact that the basis sets for the high-level energy refinement are different. The basis set for the high-level energy refinement employed in the QCISD(T):BH&HLYP method is cc-pVTZ in contrast to the 6-311++G(2df,p) basis set in the QCISD(T):MPW1K method. However, it seems that the basis set does not significantly affect the predicted reaction energies. For instance, the MADs of predicted

TABLE 1: QCISD(T)/cc-pVTZ and IMOMO (QCISD(T)/cc-pVTZ:BH&HLYP/cc-pVDZ) Reaction Energies (ΔE), Classical Barrier Heights ($\Delta V^{\ddagger}$), Absolute Deviations ($\Delta\Delta E$), and Mean Absolute Deviations (MAD) in kcal/mol

	ΔE			$\Delta V^{\ddagger}$		
reactions	QCISD(T)[a]	IMOMO[b]	$\Delta\Delta E$[c]	QCISD(T)	IMOMO	$\Delta\Delta E$
$O + H-CH_2CH_3$	5.10	4.42	0.68	12.77	12.72	0.05
$O + H-CH_2CH_2CH_3$	5.58	5.04	0.54	12.76	12.88	0.12
$O + H-CH(CH_3)_2$	2.58	1.15	1.43	10.08	10.00	0.08
$O + H-CH_2F$	4.23	3.83	0.40	14.16	13.96	0.20
$O + H-CHF_2$	4.47	3.96	0.51	14.91	14.65	0.26
$O + H-CF_3$	9.44	9.32	0.12	19.16	19.12	0.04
$O + H-CH_2C_3H_7$	5.43	4.95	0.48	12.59	12.81	0.22
$O + H-CH(CH_3)C_2H_5$	2.75	1.37	1.38	9.49	9.23	0.26
$O + H-C(CH_3)_3$	0.74	−1.53	2.27	7.91	7.91	0.00
MAD			0.87			0.14

[a] QCISD(T) denotes that the data are calculated at the QCISD(T)/cc-pVTZ// BH&HLYP/cc-pVDZ level of theory. [b] IMOMO denotes that the data are calculated at the QCISD(T):BH&HLYP level of theory as described in the electronic structure calculation section. [c] Absolute deviation = $\Delta\Delta E = |\Delta E\ (\mathrm{QCISD(T)}) - \Delta E(\mathrm{IMOMO})|$.

TABLE 2: MP4/cc-pVTZ and IMOMO (MP4/cc-pVTZ:BH&HLYP/cc-pVDZ) Reaction Energies (ΔE), Classical Barrier Heights ($\Delta V^{\ddagger}$), Absolute Deviations ($\Delta\Delta E$), and Mean Absolute Deviations (MAD) in kcal/mol

	ΔE			$\Delta V^{\ddagger}$		
reactions	MP4[a]	IMOMO[b]	$\Delta\Delta E$[c]	MP4	IMOMO	$\Delta\Delta E$
$O + H-CH_2CH_3$	4.75	4.01	0.74	12.14	12.00	0.14
$O + H-CH_2CH_2CH_3$	5.29	4.63	0.66	12.13	12.16	0.03
$O + H-CH(CH_3)_2$	2.29	0.74	1.55	9.56	9.28	0.28
$O + H-CH_2F$	3.98	3.42	0.56	13.61	13.24	0.37
$O + H-CHF_2$	4.44	3.55	0.89	14.53	13.93	0.61
$O + H-CF_3$	9.47	8.91	0.56	18.51	18.40	0.11
$O + H-CH_2C_3H_7$	5.14	4.54	0.60	11.97	12.09	0.12
$O + H-CH\ (CH_3)C_2H_5$	2.50	0.96	1.54	9.01	8.51	0.50
$O + H-C(CH_3)_3$	0.54	−1.94	2.48	7.52	7.19	0.33
MAD			1.07			0.28

[a] MP4 denotes that the data are calculated at the MP4/cc-pVTZ// BH&HLYP/cc-pVDZ level of theory. [b] IMOMO denotes that the data are calculated at the MP4:BH&HLYP level of theory as described in the electronic structure calculation section. [c] Absolute deviation = $\Delta\Delta E = |\Delta E(\mathrm{MP4}) - \Delta E(\mathrm{IMOMO})|$.

reaction energies from the QCISD(T):BH&HLYP and QCISD(T):MPW1K methods are 0.87 and 0.86 kcal/mol, respectively; the MAD of predicted reaction energies of the MP4:BH&HLYP and MP4:MPW1K methods are 1.07 and 1.06 kcal/mol, respectively. The predicted barrier heights, in contrast to the reaction energies, are relevant to the basis sets. The MADs of the predicted barrier heights at the QCISD(T):BH&HLYP, QCISD(T):MPW1K, MP4:BH&HLYP, and MP4:MPW1K levels of theory are 0.14, 0.29, 0.28, and 0.38 kcal/mol, respectively. From the above discussion we can see that all the IMOMO methods employed in this study can provide a good estimation of reaction energies and barrier heights; moreover, the QCISD(T):BH&HLYP method provides the best estimation among all the IMOMO methods.

To show the validity of the IMOMO method for the present reaction class, we calculated the thermal rate constants of the reactions listed above using the IMOMO energies and compared the calculated rate constants with available experimental data.[30−38] The Arrhenius plots of the rate constants for reactions R1−R9 are shown in Figures 1−9, respectively.

TABLE 3: MP2/cc-pVQZ and IMOMO (MP2/cc-pVQZ:BH&HLYP/cc-pVDZ) Reaction Energies (ΔE), Classical Barrier Heights ($\Delta V^{\ddagger}$), Absolute Deviations ($\Delta\Delta E$), and Mean Absolute Deviations (MAD) in kcal/mol

	ΔE			$\Delta V^{\ddagger}$		
reactions	MP2[a]	IMOMO[b]	$\Delta\Delta E$[c]	MP2	IMOMO	$\Delta\Delta E$
$O + H-CH_2CH_3$	1.10	0.33	0.77	10.37	9.93	0.44
$O + H-CH_2CH_2CH_3$	1.79	0.94	0.85	10.49	10.09	0.40
$O + H-CH(CH_3)_2$	−1.23	−2.95	1.72	8.01	7.21	0.80
$O + H-CH_2F$	0.56	−0.26	0.82	12.25	11.17	1.08
$O + H-CHF_2$	1.00	−0.13	1.13	13.88	11.86	2.02
$O + H-CF_3$	5.84	5.23	0.61	17.62	16.33	1.29
$O + H-CH_2C_3H_7$	1.64	0.86	0.78	10.37	10.02	0.35
$O + H-CH\ (CH_3)C_2H_5$	−0.92	−2.73	1.81	7.75	6.44	1.31
$O + H-C(CH_3)_3$	−2.76	−5.63	2.87	6.18	5.12	1.06
MAD			1.26			0.97

[a] MP2 denotes that the data are calculated at the MP2/cc-pVQZ// BH&HLYP/cc-pVDZ level of theory. [b] IMOMO denotes that the data are calculated at the MP2:BH&HLYP level of theory as described in the electronic structure calculation section. [c] Absolute deviation = $\Delta\Delta E = |\Delta E(\mathrm{MP2}) - \Delta E(\mathrm{IMOMO})|$.

TABLE 4: QCISD(T)/6-311++G(2df,p) and IMOMO (QCISD(T)/6-311++G(2df,p):MPW1K/6-31+G(d,p)) Reaction Energies (ΔE), Classical Barrier Heights ($\Delta V^{\ddagger}$), Absolute Deviations ($\Delta\Delta E$), and Mean Absolute Deviations (MAD) in kcal/mol

	ΔE			$\Delta V^{\ddagger}$		
reactions	QCISD(T)[a]	IMOMO[b]	$\Delta\Delta E$[c]	QCISD(T)	IMOMO	$\Delta\Delta E$
$O + H-CH_2CH_3$	4.44	3.79	0.65	12.38	12.33	0.05
$O + H-CH_2CH_2CH_3$	4.73	4.02	0.71	12.36	12.53	0.16
$O + H-CH(CH_3)_2$	1.86	0.45	1.41	9.51	9.51	0.00
$O + H-CH_2F$	4.17	4.08	0.09	14.40	14.49	0.09
$O + H-CHF_2$	4.24	3.99	0.25	15.04	15.48	0.44
$O + H-CF_3$	9.01	8.63	0.38	19.25	20.07	0.82
$O + H-CH_2C_3H_7$	4.88	4.19	0.69	12.19	12.42	0.23
$O + H-CH(CH_3)C_2H_5$	2.08	0.63	1.45	8.98	9.39	0.41
$O + H-C(CH_3)_3$	−0.02	−2.17	2.15	7.04	7.45	0.41
MAD			0.86			0.29

[a] QCISD(T) denotes that the data are calculated at the QCISD(T)/6-311++G(2df,p)// MPW1K/6-31+G(d,p) level of theory. [b] IMOMO denotes that the data are calculated at the QCISD(T):MPW1K level of theory as described in the electronic structure calculation section. [c] Absolute deviation = $\Delta\Delta E = |\Delta E(\mathrm{QCISD(T)}) - \Delta E(\mathrm{IMOMO})|$.

From these figures, we can see that all the rate constants calculated from the IMOMO energies are very close to those from the full high-level energies. The rate constants calculated at the QCISD(T)/6-311++G(2df,p) level of theory are different from those calculated at the QCISD(T)/cc-pVTZ level of theory. The difference of rate constants between the two levels mainly comes from the difference of barrier heights that are originated from the difference of the size of basis functions for the correlation energy calculation in the IMOMO method.

We also compared the calculated rate constants with the available experimental data or those derived either from fitting to a complex reaction mechanism or other experimental data in Figures 1−9. From these figures, we can see that the theoretical predictions are in good agreement with the experimental results at high temperatures. At low temperatures, the calculated rate constants are still close to the experimental data despite the fact that the calculated rate constants are generally smaller than the experimental data. This may be caused by the underestimation of the tunneling effects of the Eckart method and can be

TABLE 5: MP4/6-311++G(2df,p) and IMOMO (MP4/6-311++G(2df,p):MPW1K/ 6-31+G(d,p)) Reaction Energies (ΔE), Classical Barrier Heights ($\Delta V^{\ddagger}$), Absolute Deviations ($\Delta\Delta E$), and Mean Absolute Deviations (MAD) in kcal/mol

	ΔE			$\Delta V^{\ddagger}$		
reactions	MP4[a]	IMOMO[b]	$\Delta\Delta E$[c]	MP4	IMOMO	$\Delta\Delta E$
$O + H{-}CH_2CH_3$	4.14	3.43	0.71	12.17	11.83	0.34
$O + H{-}CH_2CH_2CH_3$	4.47	3.66	0.82	12.14	12.03	0.11
$O + H{-}CH(CH_3)_2$	1.61	0.09	1.52	9.64	9.01	0.63
$O + H{-}CH_2F$	3.98	3.72	0.26	14.40	13.99	0.41
$O + H{-}CHF_2$	4.26	3.63	0.63	15.34	14.98	0.36
$O + H{-}CF_3$	9.10	8.27	0.83	18.94	19.57	0.63
$O + H{-}CH_2C_3H_7$	4.64	3.83	0.81	11.99	11.92	0.07
$O + H{-}CH\ (CH_3)C_2H_5$	1.88	0.26	1.62	9.13	8.89	0.24
$O + H{-}C(CH_3)_3$	−0.17	−2.53	2.36	7.55	6.95	0.60
MAD			1.06			0.38

[a] MP4 denotes that the data are calculated at the MP4/6-311++G(2df,p)//MPW1K/ 6-31+G(d,p) level of theory. [b] IMOMO denotes that the data are calculated at the MP4: MPW1K level of theory as described in the electronic structure calculation section. [c] Absolute deviation = $\Delta\Delta E = |\Delta E(\mathrm{MP4}) - \Delta E(\mathrm{IMOMO})|$.

TABLE 6: MP2/6-311++G(3df,2pd) and IMOMO (MP2/6-311++G(3df,2pd):MPW1K/6-31+G(d,p)) Reaction Energies (ΔE), Classical Barrier Heights ($\Delta V^{\ddagger}$), Absolute Deviations ($\Delta\Delta E$), and Mean Absolute Deviations (MAD) in kcal/mol

	ΔE			$\Delta V^{\ddagger}$		
reactions	MP2[a]	IMOMO[b]	$\Delta\Delta E$[c]	MP2	IMOMO	$\Delta\Delta E$
$O + H{-}CH_2CH_3$	0.65	−0.34	0.99	10.64	9.86	0.79
$O + H{-}CH_2CH_2CH_3$	1.02	−0.11	1.13	10.65	10.05	0.59
$O + H{-}CH(CH_3)_2$	−1.59	−3.67	2.08	8.48	7.04	1.44
$O + H{-}CH_2F$	0.29	−0.05	0.33	13.06	12.02	1.05
$O + H{-}CHF_2$	0.71	−0.14	0.85	14.26	13.01	1.25
$O + H{-}CF_3$	5.49	4.51	0.99	17.58	17.60	0.02
$O + H{-}CH_2C_3H_7$	1.14	0.07	1.07	10.53	9.95	0.58
$O + H{-}CH\ (CH_3)C_2H_5$	−1.29	−3.50	2.21	8.03	6.92	1.12
$O + H{-}C(CH_3)_3$	−3.04	−6.29	3.25	6.84	4.98	1.86
MAD			1.43			0.97

[a] MP2 denotes that the data are calculated at the MP2/6-311++G-(3df,2pd)//MPW1K/ 6-31+G(d,p) level of theory. [b] IMOMO denotes that the data are calculated at the MP2:MPW1K level of theory as described in the electronic structure calculation section. [c] Absolute deviation = $\Delta\Delta E = |\Delta E(\mathrm{MP2}) - \Delta E(\mathrm{IMOMO})|$.

TABLE 7: High/6-311++G(2df,p) and IMOMO (High/6-311++G(2df,p):MPW1K/6-31+G(d,p)) CPU Hours, Where High Is the QCISD(T) or MP4 Method

	CPU time			
reactions	QCISD(T)	IMOMO (QCISD(T): MPW1K)	MP4	IMOMO (MP4: MPW1K)
$O + H{-}CH_2CH_3$	4.06	3.74	1.46	2.23
$O + H{-}CH_2C_2H_5$	32.58	5.53	15.71	4.02
$O + H{-}CH_2C_3H_7$	115.72	11.10	49.44	9.59

improved by choosing the SCT tunneling method. Thus, the IMOMO method is a good approximation in predicting the barrier heights in the calculation of rate constants for the O + H−R → OH + R• reaction class.

To show the efficiency of the IMOMO approach, we listed the CPU time required for the IMOMO calculation and the high-level energy refinements in Table 7. In this table, the CPU time of the IMOMO calculation includes the optimization time of both the real and model reaction systems at the low level of theory and that of the high-level energy refinement of the model reaction system; the CPU time of the high-level (QCISD(T) and MP4) methods only include the CPU time of the energy refinement at the high level of theory for the real systems. From Table 7, we can see that the CPU time of the high-level energy refinement of real reaction systems increases dramatically with the size of molecules. For the C_2H_6 molecule, the CPU time of the high-level calculations are close to those of the IMOMO calculations. However, the CPU time of the QCISD(T)/cc-pVTZ and MP4/cc-pVTZ energy refinement is larger than that of the IMOMO calculation by factors of 10 and 5, respectively, for the C_4H_{10} molecule. As the size of the molecules increases, this factor will rise more quickly. In contrast, the CPU time of IMOMO calculations rises much more slowly.

IV. Summary

We presented in this work an IMOMO study on the O + H−R → OH + R• reaction class. The mean absolute deviations of the predicted barrier heights of the IMOMO (QCISD(T):BH&HLYP), IMOMO (MP4:BH&HLYP), IMOMO (QCISD-(T):MPW1K), and IMOMO (MP4:MPW1K) methods are 0.14, 0.28, 0.29, and 0.38 kcal/mol, respectively, compared with the exact corresponding high-level energy refinement. The MADs of the predicted reaction energies of the same IMOMO methods are 0.87, 1.07, 0.86, and 1.06 kcal/mol, respectively. The predicated rate constants from the IMOMO energies are in good agreement with those from the full high-level energies and with the available experimental data. In particular, the IMOMO approach requires many little computational demands compared to the exact high-level energy refinement. These results imply that the IMOMO approach, especially for large molecular systems, is an efficient and practical tool in predicting energies of the O + H−R → OH + R• reaction class.

Acknowledgment. This work was supported by the National Natural Science Foundation of China (20373007) and the Foundation for basic research by the Beijing Institute of Technology.

References and Notes

(1) Maseras, F.; Morokuma, K. *J. Comput. Chem.* **1995**, *16*, 1170.

(2) Svensson, M.; Humbel, S.; Froese, R. D. J.; Matsubara, T.; Sieber, S.; Morokuma, K. *J. Phys. Chem.* **1996**, *100*, 19357.

(3) Humbel, S.; Sieber, S.; Morokuma, K. *J. Chem. Phys.* **1996**, *105*, 1959.

(4) Svensson, M.; Humbel, S.; Morokuma, K. *J. Chem. Phys.* **1996**, *105*, 3654.

(5) Froese, R. D. J.; Morokuma, K. *Chem. Phys. Lett.* **1996**, *263*, 393.

(6) Humbel, S. *THEOCHEM* **1999**, *461*, 153.

(7) Truong, T. N.; Duncan, W. T.; Tirtowidjojo, M. *Phys. Chem. Chem. Phys.* **1999**, *1*, 1061.

(8) Truong, T. N. *J. Chem. Phys.* **2000**, *113*, 4957.

(9) Zhang, S. W.; Truong, T. N. *J. Phys. Chem. A* **2003**, *107*, 1138.

(10) Truong, T. N.; Truong, T.-T. T. *Chem. Phys. Lett.* **1999**, *314*, 529.

(11) Truong, T. N.; Maity, D. K.; Truong, T.-T. T. *J. Chem. Phys.* **2000**, *112*, 24.

(12) Garrett, B. C.; Truhlar, D. G. *J. Chem. Phys.* **1979**, *70*, 1593.

(13) Truhlar, D. G.; Garrett, B. C. *Acc. Chem. Res.* **1980**, *13*, 440.

(14) Truhlar, D. G.; Isaacson, A. D.; Skodje, R. T.; Garrett, B. C. *J. Phys. Chem.* **1982**, *86*, 2252.

(15) Truhlar, D. G.; Garrett, B. C. *Annu. Rev. Phys. Chem.* **1984**, *35*, 159.

(16) Truhlar, D. G.; Isaacson, A. D.; Garrett, B. C. Generalized transition state theory. In *Theory of Chemical Reaction Dynamics*; Baer, M., Ed.; CRC Press: Boca Raton, FL, 1985; Vol. 4, p 65.

(17) Truhlar, D. G.; Garrett, B. C. *J. Chem. Phys.* **1987**, *84*, 365.

(18) Tucker, S. C.; Truhlar, D. G. In *New Theoretical Concepts for Understanding Organic Reactions*; Bertran, J., Csizmadia, I. G., Eds.; Kluwer Academic: Dordrecht, 1989.

(19) Lu, D.-h.; Truong, T. N.; Melissas, V. S.; Lynch, G. C.; Liu, Y. P.; Garrett, B. C.; Steckler, R.; Isaacson, A. D.; Rai, S. N.; Hancock, G. C.; Lauderdale, J. G.; Joseph, T.; Truhlar, D. G. *Comput. Phys. Commun.* **1992**, *71*, 235.

(20) Truhlar, D. G.; Garrett, B. C.; Klippenstein, S. J. *J. Phys. Chem.* **1996**, *100*, 12771.

(21) Truong, T. N.; Truhlar, D. G. *J. Chem. Phys.* **1990**, *93*, 1761.

(22) Truong, T. N.; Duncan, W. T. *J. Chem. Phys.* **1994**, *101*, 7408.

(23) Duncan, W. T.; Truong, T. N. *J. Chem. Phys.* **1995**, *103*, 9642.

(24) Lynch, B. J.; Fast, P. L.; Harris, M.; Truhlar, D. G. *J. Phys. Chem. A* **2000**, *104*, 4811.

(25) Lynch, B. J.; Truhlar, D. G. *J. Phys. Chem. A* **2001**, *105*, 2936.

(26) Lynch, B. J.; Truhlar, D. G. *J. Phys. Chem. A* **2002**, *106*, 842.

(27) Lynch, B. J.; Zhao, Y.; Truhlar, D. G. *J. Phys. Chem. A* **2003**, *107*, 1384.

(28) Li, Q. S.; Xu, X. D.; Zhang, S. W. *Chem. Phys. Lett.* **2004**, *384*, 20.

(29) Frisch, M. J.; Trucks, G. W.; Schlegel, H. B.; Scuseria, G. E.; Robb, M. A.; Cheeseman, J. R.; Zakrzewski, V. G.; Montgomery, J. A.; Stratmann, R. E.; Burant, J. C.; Dapprich, S.; Millam, J. M.; Daniels, A. D.; Kudin, K. N.; Strain, M. C.; Farkas, O.; Tomasi, J.; Barone, V.; Cossi, M.; Cammi, R.; Mennucci, B.; Pomelli, C.; Adamo, C.; Clifford, S.; Ochterski, J.; Petersson, G. A.; Ayala, P. Y.; Cui, Q.; Morokuma, K.; Malick, D. K.; Rabuck, A. D.; Raghavachari, B.; Foresman, J. B.; Cioslowski, J.; Ortiz, J. V.; Stefanov, B.; Liu, G.; Liashenko, A.; Piskorz, P.; Komaromi, I.; Gomperts, R.; Martin, R. L.; Fox, D. J.; Keith, T.; A1-Laham, M. A.; Peng, C. Y.; Nanayakkara, A.; GonZalez, C.; Challacombe, M.; Gill, P. M. W.; Johnson, B. G.; Chen, W.; Wong, M. W.; Andres, J. L.; Head-Gordon, M.; Replogle, E. S.; Pople, J. A. *Gaussian 98*, revision A.9; Gaussian Inc.: Pittsburgh, PA, 1998.

(30) Miyoshi, A.; Ohmori, K.; Tsuchiya, K.; Matsui, H. *Chem. Phys. Lett.* 1993**,** *204*, 241.

(31) Mahmud, K.; Marshall, P.; Fontijn, A. *J. Chem. Phys.* **1988**, *88*, 2393.

(32) Tsang, W. *J. Phys. Chem. Ref. Data* **1988**, *17*, 887.

(33) Cohen, N.; Westberg, K. R. *Int. J. Chem. Kinet.* **1986**, *18*, 99.

(34) parsamyan, N. I.; Nalbandyan, A. B. *Arm. Khim. Zh.* **1968**, *21*, 1.

(35) Medhurst, L. J.; Fleming, J.; Nelson, H. H. *Chem. Phys. Lett.* **1997**, *266*, 607.

(36) Jourdain, J. L.; Poulet, G.; Barassin, J.; Le Bras, G.; Combourieu, J. *Pollut. Atoms.* **1977**, *75*, 256.

(37) Tsang, W. *J. Phys. Chem. Ref. Data* **1990**, *19*, 1.

(38) Herron, J. T.; Huie, R. E. *J. Phys. Chem.* **1969**, *73*, 3327.